

## Supporting Information

### **Atomic Dispersion Platinum Anchored on Porous Alumina Sheets as an Efficient Catalyst for Diboration of Alkynes**

Huishan Shang,<sup>a</sup> Wenxing Chen,<sup>\*a</sup> Zhuoli Jiang,<sup>a</sup> Danni Zhou,<sup>a</sup> and Jiatao Zhang<sup>\*a</sup>

a. Beijing Key Laboratory of Construction Tailorable Advanced Functional Materials and Green Applications, School of Materials Science and Engineering, Beijing Institute of Technology, Beijing 100081, China.

\* Corresponding author. E-mail: wxchen@bit.edu.cn, zhangjt@bit.edu.cn.

## **Table of contents**

- 1. Experiment detail**
- 2. Supplementary Figures and Tables**
- 3. References**

### **1. Experiment detail**

#### **Materials**

Analytical grade Aluminium chloride ( $\text{AlCl}_3$ ), Magnesium powder (Mg), 1-Butanesulfonic acid sodium salt (BSAC) and Chloroplatinic acid ( $\text{H}_2\text{PtCl}_6 \cdot 6\text{H}_2\text{O}$ ) were obtained from Sinopharm Chemical Reagent Co.,Ltd. bis(pinacolato)diboron ( $\text{B}_2\text{pin}_2$ ) was purchased from Sigma-Aldrich. Methylbenzene and phenylacetylene were purchased from Innochem. All the materials were used as received without further purification.

#### **Synthesis of defect porous $\text{Al}_2\text{O}_3$ nanosheets (dp- $\text{Al}_2\text{O}_3$ )**

$\text{AlCl}_3$  (1 mmol, 133.3 mg) was dissolved in deionized water (10 mL) and then mixed with an aqueous solution of Mg powder (1.5 mmol, 36.5 mg), BSAC (1.5mmol, 0.2g) in deionized water (20 mL). After vigorous stirring for 30 min at ambient temperature, the mixture was transferred into a 50 mL Teflon-lined stainless-steel autoclave and heated at 200 °C for 3 h. The white product was collected via centrifugation and further washed with deionized water and ethanol for two times, respectively. After vacuum freeze-drying, the AlOOH nanosheets were obtained. Then, the resulting powder was placed into the tube furnace and heated to the desired temperature 500 °C for 120 min at the heating rate of 2 °C/min in Air. After cooling to room temperature, the dp- $\text{Al}_2\text{O}_3$  was used for characterization and further preparation without further purification.

#### **Synthesis of the Pt/dp- $\text{Al}_2\text{O}_3$ catalyst.**

The as-synthesized  $\text{Al}_2\text{O}_3$  (100.0 mg) were first dispersed in 20 mL ethanol under ultrasonic vibration. A  $\text{H}_2\text{PtCl}_6 \cdot 6\text{H}_2\text{O}$  solution (1mg/ml) was next added dropwise into the  $\text{Al}_2\text{O}_3$  dispersion under stirring at ambient temperature. After continuous stirring

overnight, the suspension was centrifuged. The recovered solid was then dried in vacuum oven and reduced in 5% H<sub>2</sub>/N<sub>2</sub> at 200 °C for 2 h to afford the Pt/dp-Al<sub>2</sub>O<sub>3</sub> catalyst for further characterization and catalysis test.

### **Synthesis of the Pt NPs/c-Al<sub>2</sub>O<sub>3</sub> catalyst.**

The Pt NPs/c-Al<sub>2</sub>O<sub>3</sub> was synthesized through the same procedure of the fabrication of Pt/dp-Al<sub>2</sub>O<sub>3</sub> catalyst except with a commercial Al<sub>2</sub>O<sub>3</sub> support instead.

### **Characterization**

Powder X-ray diffraction patterns of samples were recorded on a Bruker D8 Advance powder X-ray diffractometer at a scanning rate of 5 °C min<sup>-1</sup> and using a Cu K $\alpha$  radiation ( $\lambda=0.15406$  Å). TEM images were recorded by a JEOL JEM 1200EX working at 100 kV. The high-resolution TEM, HAADF-STEM images the corresponding Electron energy-loss spectroscopy were recorded by a FEI Tecnai G2 F20 S-Twin high-resolution transmission electron microscope working at 200 kV and on a JEOL JEM-ARM200F TEM/STEM with a spherical aberration corrector working at 300 kV. The X-ray photoelectron spectroscopy (XPS) measurements were performed with a PerkinElmer Physics PHI 5300 spectrometer using Al K $\alpha$  nonmonochromatic radiation, and the binding energy of the C1s peak at 284.8 eV was taken as an internal reference.

### **Catalysis testing**

In a typical procedure, alkynes (0.5 mmol, 0.5 equiv.), B<sub>2</sub>pin<sub>2</sub> (0.5 mmol), Pt species catalysts (Pt 0.0005 equiv.) and methylbenzene (3 mL) were sequentially added in a 20 mL standard Schlenk tube equipped with a stir bar, then the mixture was heated at 100 °C and vigorously stirred for 6 hours. When the reaction was over, the yield of reaction was determined by GC and GC-MS with dodecane as the internal standard. The TOF values were calculated upon completion of reactions and based on the total Pt loading in the catalysts.

### **XAFS measurements**

XAFS spectra at Pt L<sub>3</sub>-edge were collected at the 1W1B station in Beijing Synchrotron Radiation Facility in a fluorescence mode, Pt foil, PtO<sub>2</sub> were used as references. The k<sup>3</sup>-weighted EXAFS spectra were obtained by subtracting the post-edge background from the overall absorption and then normalizing with respect to the edge-jump step.

Subsequently,  $k^3$ -weighted  $\chi(k)$  data in the  $k$  space ranging from 2.0-12.0  $\text{\AA}^{-1}$  were Fourier transformed to real (R) space using hanning windows ( $dk = 1.0 \text{\AA}^{-1}$ ) to separate the EXAFS contributions from different coordination shell.

### **XAFS data processing**

The acquired EXAFS data were processed according to the standard procedures using the Athena and Artemis implemented in the IFEFFIT software packages. The fitting detail is described below: The acquired EXAFS data were processed according to the standard procedures using the ATHENA module implemented in the IFEFFIT software packages. The EXAFS spectra were obtained by subtracting the post-edge background from the overall absorption and then normalizing with respect to the edge-jump step. Subsequently, the  $\chi(k)$  data were Fourier transformed to real (R) space using a hanning windows ( $dk=1.0 \text{\AA}^{-1}$ ) to separate the EXAFS contributions from different coordination shells. To obtain the quantitative structural parameters around central atoms, least-squares curve parameter fitting was performed using the ARTEMIS module of IFEFFIT software packages.<sup>1</sup> The following EXAFS equation was used:

$$\chi(k) = \sum_j \frac{N_j S_0^2 F_j(k)}{k R_j^2} \exp[-2k^2 \sigma_j^2] \exp\left[-\frac{2R_j}{\lambda(k)}\right] \sin[2k R_j + \phi_j(k)]$$

$S_0^2$  is the amplitude reduction factor,  $F_j(k)$  is the effective curved-wave backscattering amplitude,  $N_j$  is the number of neighbors in the  $j^{\text{th}}$  atomic shell,  $R_j$  is the distance between the X-ray absorbing central atom and the atoms in the  $j^{\text{th}}$  atomic shell (backscatterer),  $\lambda$  is the mean free path in  $\text{\AA}$ ,  $\phi_j(k)$  is the phase shift (including the phase shift for each shell and the total central atom phase shift),  $\sigma_j$  is the DebyeWaller parameter of the  $j^{\text{th}}$  atomic shell (variation of distances around the average  $R_j$ ). The functions  $F_j(k)$ ,  $\lambda$  and  $\phi_j(k)$  were calculated with the ab initio code FEFF8.2. The additional details for EXAFS simulations are given below. The coordination numbers of model samples (Pt foil) were fixed as the nominal values. The obtained  $S_0^2$  was fixed in the subsequent fitting of atomic dispersed Pt samples. While the internal atomic distances  $R$ , Debye-Waller factor  $\sigma^2$ , and the edge-energy shift  $\Delta E_0$  were allowed to run freely.

## 2. Supplementary Figures and Tables

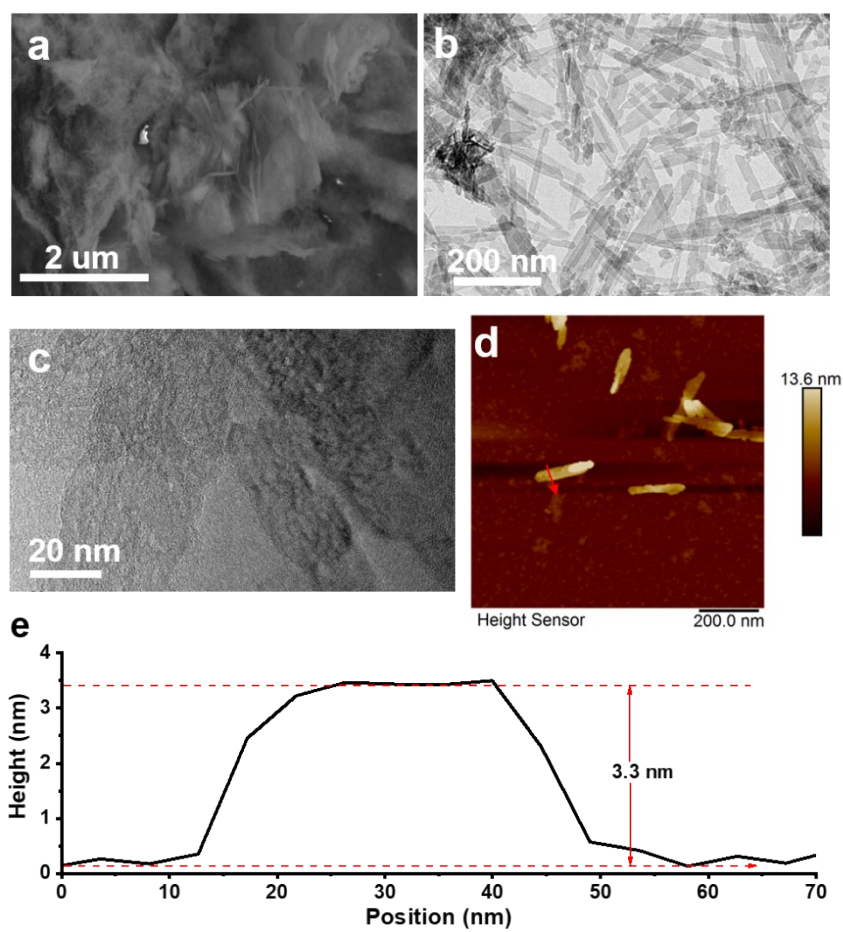


**Fig. S1.** (a) SEM, (b) TEM, (c) HRTEM (d) AFM characterizations of AlOOH, and (e) The corresponding height profiles of the scans shown in the AFM image. The nanosheet morphology of AlOOH could be confirmed by SEM, TEM, HRTEM and AFM spectra.

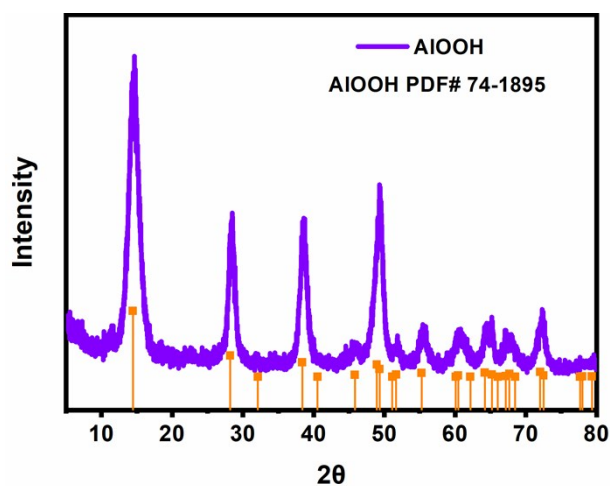


**Fig. S2.** XRD pattern of AlOOH, which suggest the phase (JCPDS No. 74-1895) with a high crystallinity.

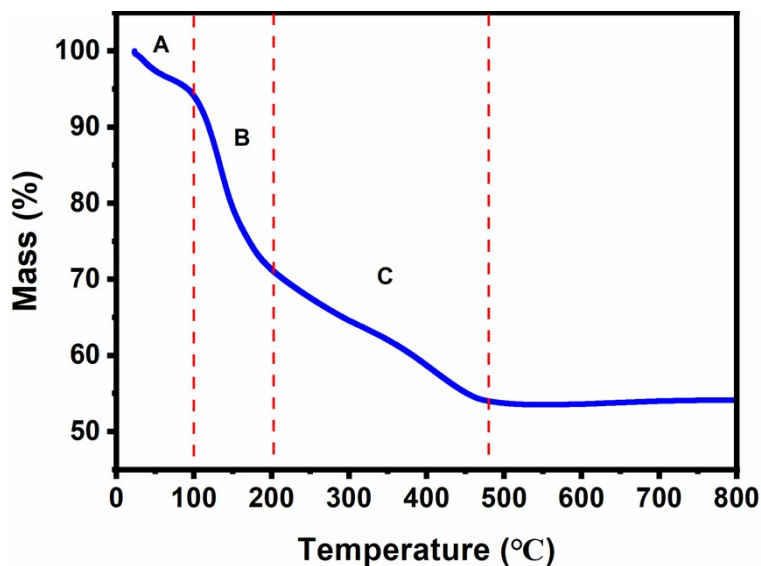


**Fig. S3.** TGA curve of AlOOH in air from 25 °C to 800 °C. TGA is used to explore the process for AlOOH thermal decomposition. The TGA curve indicates a 6 % weight loss in the temperature range of 20 °C to 100 °C in stage A, due to the evaporation of physical-absorption water. Stage B corresponds to the removal of organic molecules of BSAC, with a total weight loss of 23 %. Stage C is due to the phase transformation of boehmite to the  $\gamma$ -Al<sub>2</sub>O<sub>3</sub>, with a total weight loss of 17 %, which is consistent with the theoretical weight loss from the transition of  $\gamma$ -AlOOH to  $\gamma$ -Al<sub>2</sub>O<sub>3</sub>.<sup>2</sup> Based on the above results, 500 °C was chosen as the reasonable annealing temperature.

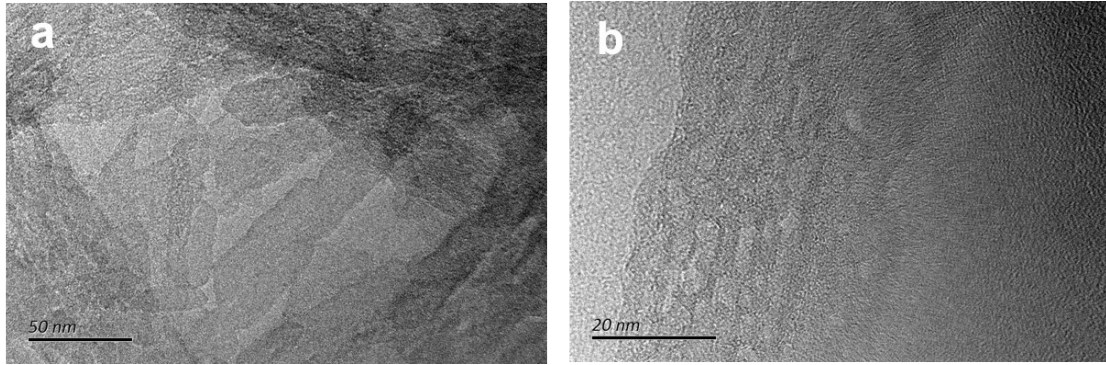


**Fig. S4. (a, b)** TEM and HRTEM images of porous defect alumina sheets. The porous structure can be seen from the TEM image.

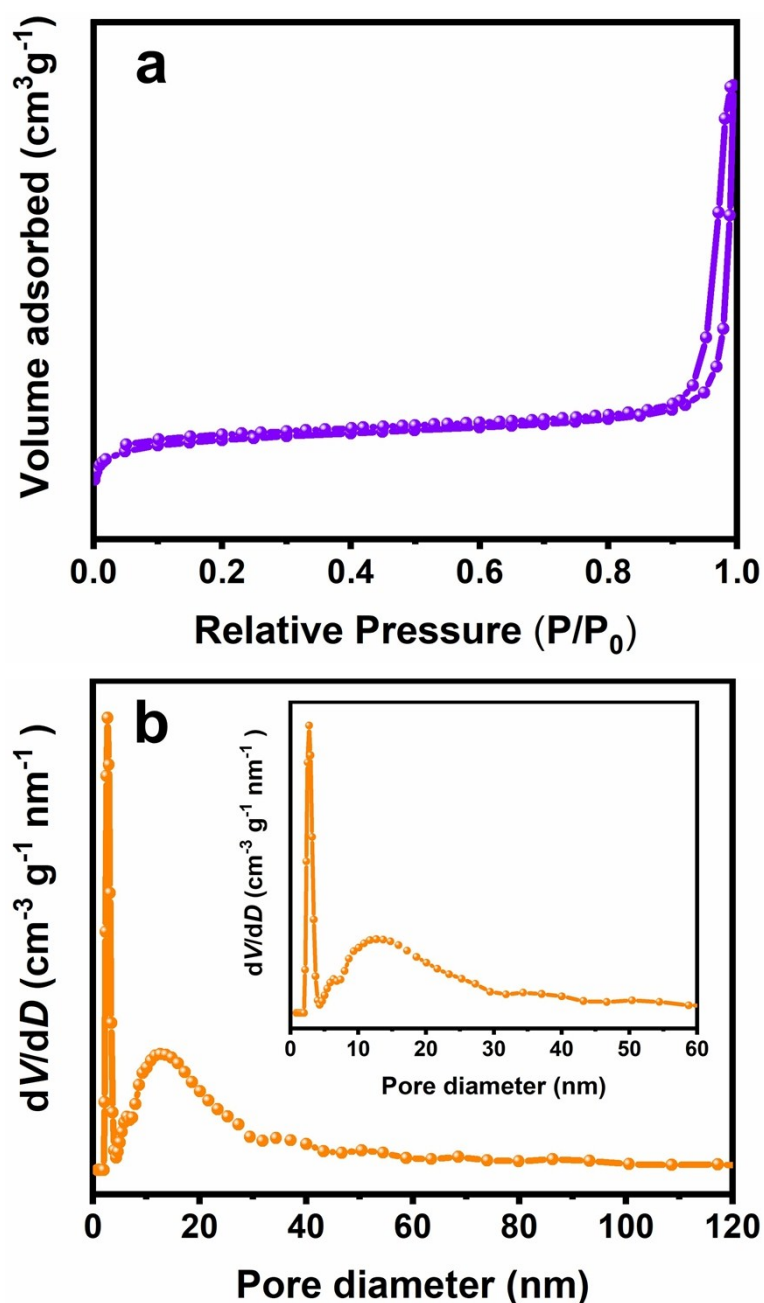


**Fig. S5.** (a)  $N_2$  adsorption-desorption isotherms of dp- $Al_2O_3$  and the corresponding pore-size distribution curve (b). The BET specific surface area of the as-prepared dp- $Al_2O_3$  calculated on the basis of the nitrogen adsorption-desorption isotherms at 77 K were determined to be  $229 \text{ m}^2 \cdot \text{g}^{-1}$ . The pore diameter distributions for dp- $Al_2O_3$  are approximately 2.7 nm and 13.3 nm in diameter, which is consistent with the TEM analysis. These results indicate that the obtained  $Al_2O_3$  possess high surface area and good porous characters.

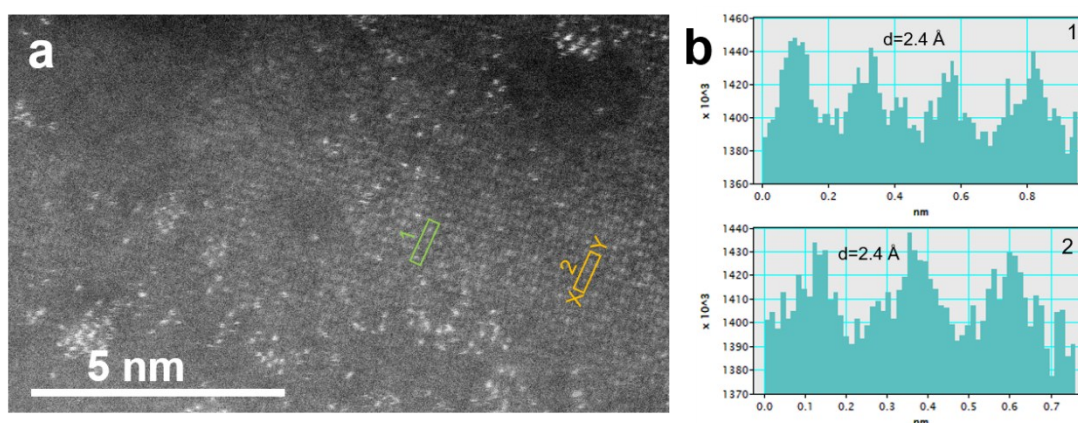


**Fig. S6.** Careful scan of HAADF-TEM on Pt/dp- $\text{Al}_2\text{O}_3$  (a) and (b) The intensity profiles of the areas labelled in (a),  $d \text{ Al}_2\text{O}_3 (311) = 2.4 \text{ \AA}$ .

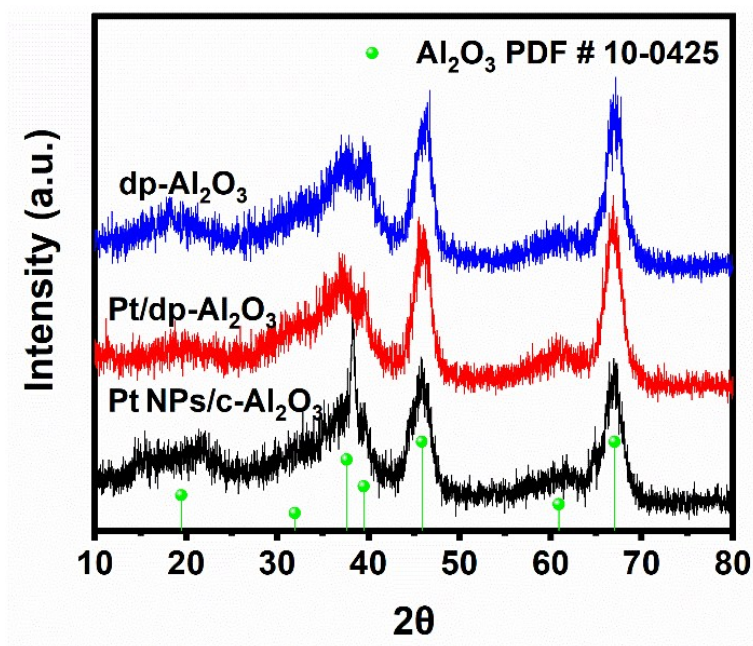


**Fig. S7.** XRD patterns of dp- $\text{Al}_2\text{O}_3$  (blue), Pt/dp- $\text{Al}_2\text{O}_3$  (red), Pt NPs/c- $\text{Al}_2\text{O}_3$  (black). As can be seen, the XRD pattern of Pt/dp- $\text{Al}_2\text{O}_3$  and Pt NPs/c- $\text{Al}_2\text{O}_3$  are similar to dp- $\text{Al}_2\text{O}_3$  without peaks attributed to Pt nanoparticles detected.

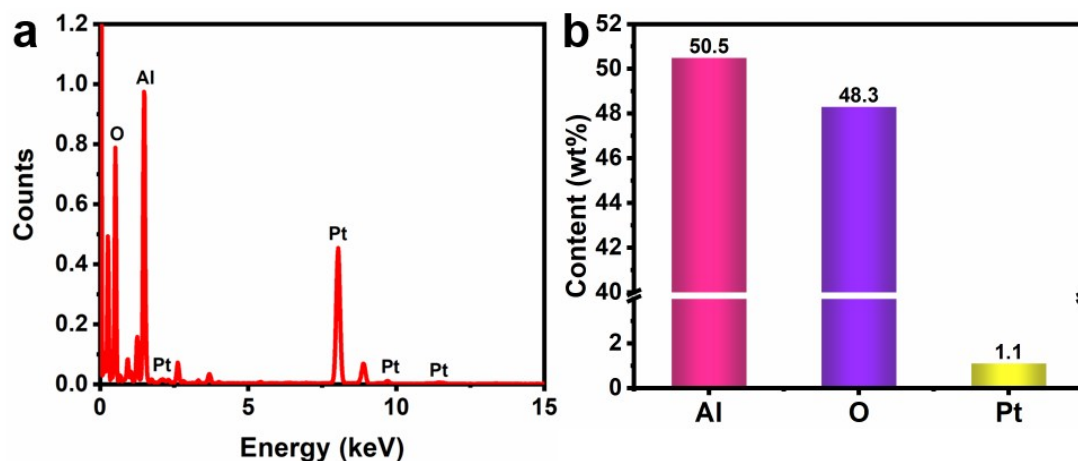


**Fig. S8.** (a) EDS spectrum of Pt/dp-Al<sub>2</sub>O<sub>3</sub>. (b) The weight content percentages of Al, O and Pt in Pt/dp-Al<sub>2</sub>O<sub>3</sub> measured by EDS analysis. The actual loading of Pt in Pt/dp-Al<sub>2</sub>O<sub>3</sub> was about 1.3 wt %, corresponding to the results of ICP-OES.

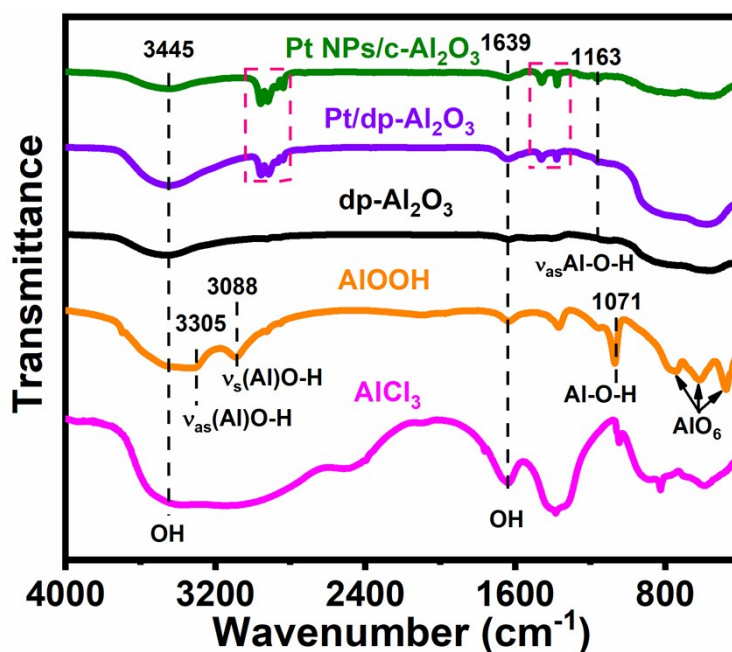


**Fig. S9.** FT-IR spectra of AlCl<sub>3</sub>, AlOOH, dp-Al<sub>2</sub>O<sub>3</sub>, Pt/dp-Al<sub>2</sub>O<sub>3</sub> and Pt NPs/c-Al<sub>2</sub>O<sub>3</sub>. As can be seen from the FT-IR spectrum, the bands at 3445 and 1639 cm<sup>-1</sup> can be assigned to the O–H vibration of hydrogen-bonded hydroxyl groups from the metal hydroxide and intercalated water molecule. The band at 1071 cm<sup>-1</sup> corresponds to the stretching vibrations of Al-O-H. Three bands at 755, 614 and 473 cm<sup>-1</sup> are characteristic of AlO<sub>6</sub>. Thermal decomposition of AlOOH at 500 °C, the band corresponding to v<sub>as</sub>(Al)-O-H, v<sub>s</sub>(Al)-O-H, Al-O-H and AlO<sub>6</sub> vanished, meanwhile new band at 1163cm<sup>-1</sup>

corresponding to the asymmetrical stretching vibration of Al-O-H appeared.<sup>3, 4</sup> Above data confirms the successful phase transformation of AlOOH to the Al<sub>2</sub>O<sub>3</sub>. The weak band in the red box may be attributed to Pt-Al related bond in Pt/dp-Al<sub>2</sub>O<sub>3</sub> and Pt NPs/c-Al<sub>2</sub>O<sub>3</sub>.

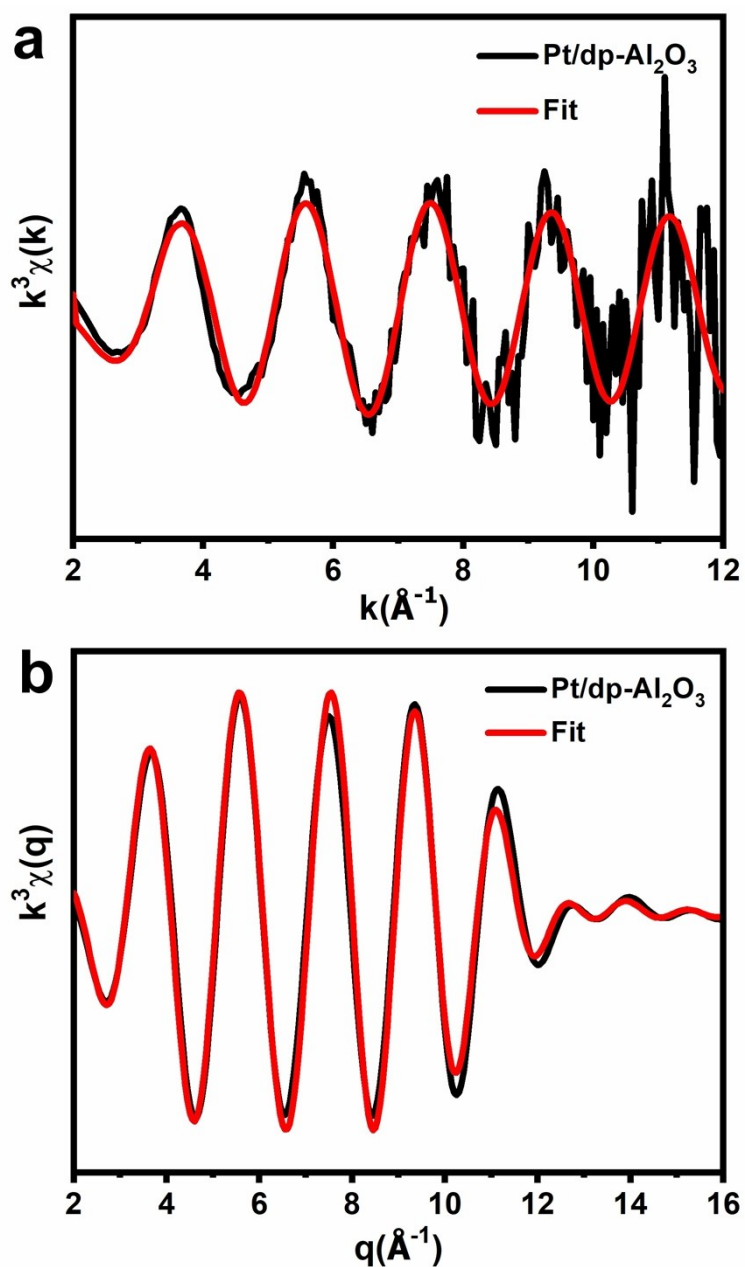


**Fig. S10.** (a) k space EXAFS fitting curves of the Pt/dp-Al<sub>2</sub>O<sub>3</sub>. (b) Inversed FT-EXAFS fitting curves of the Pt/dp-Al<sub>2</sub>O<sub>3</sub>.

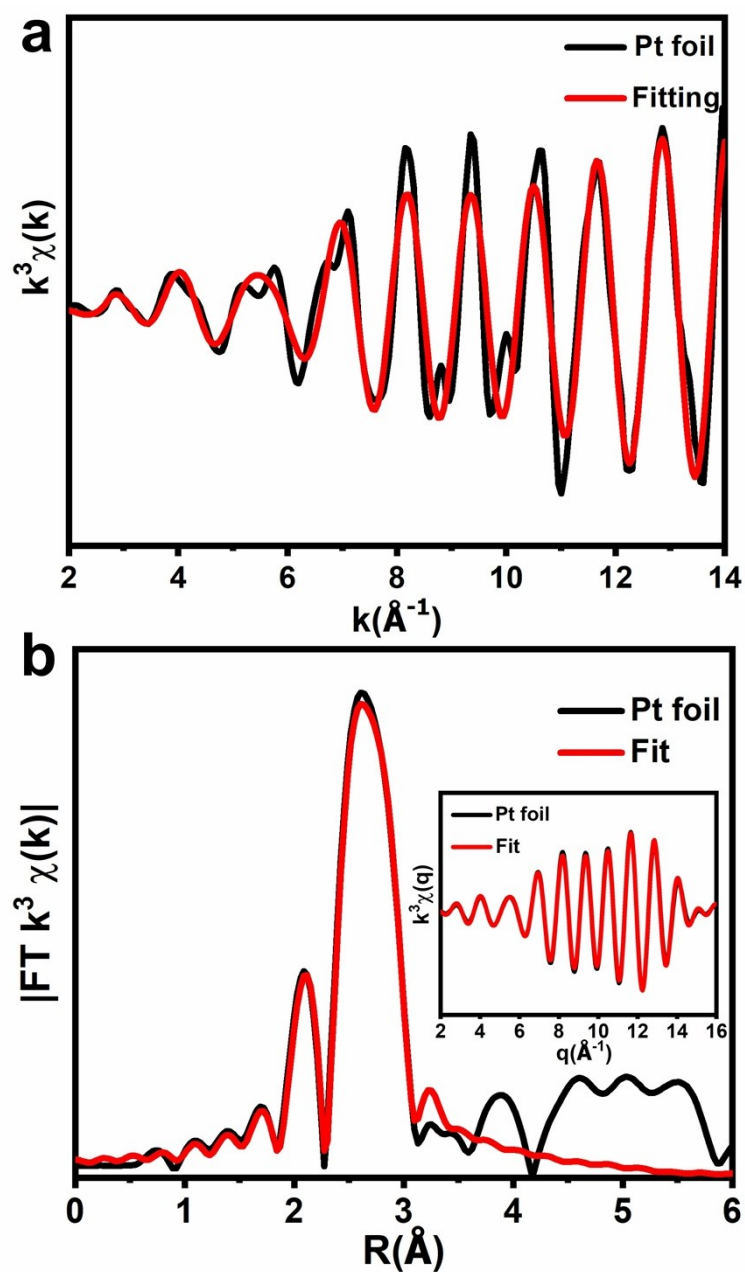


**Fig. S11** (A) k space EXAFS, (B) FT-EXAFS and inversed FT-EXAFS fitting curves of Pt foil (FT range: 2.0-12.0  $\text{\AA}^{-1}$ , fitting range: 1.5-3.5  $\text{\AA}$ ).

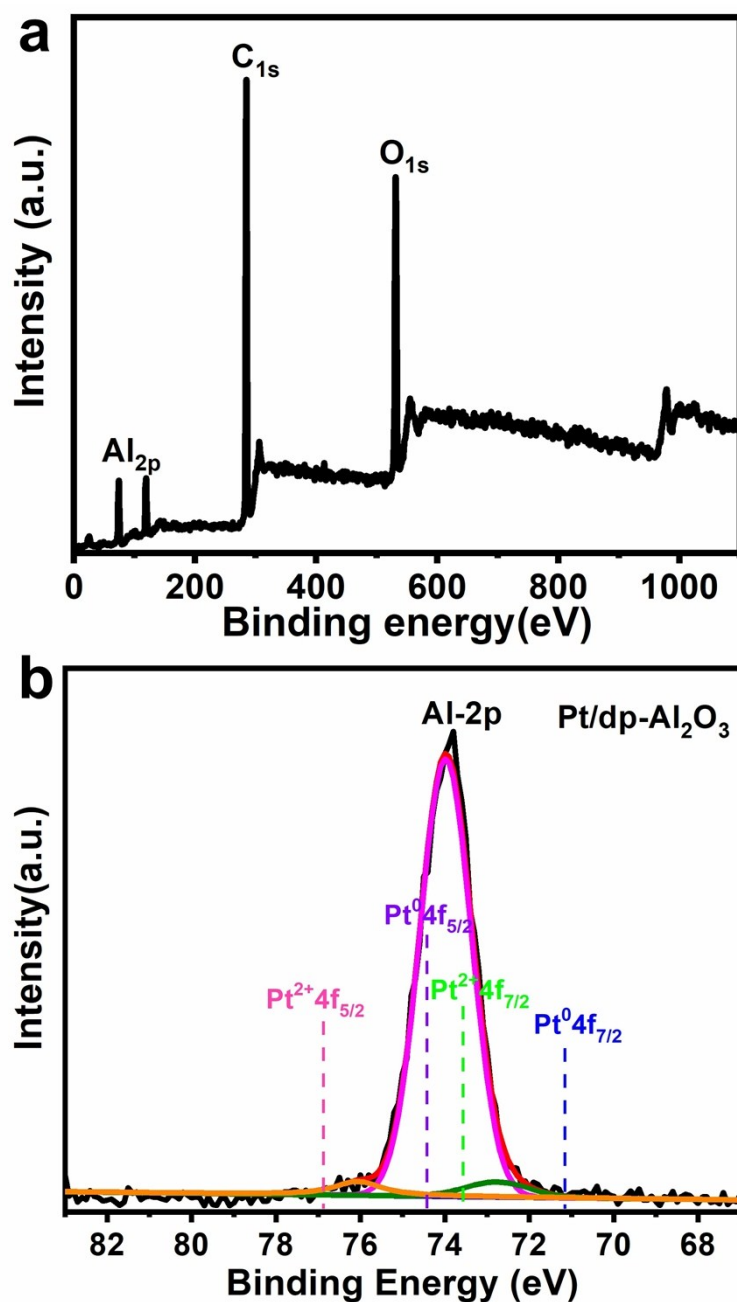


**Fig. S12.** XPS spectra for the survey scan (a) and Al 2P, Pt 4f region of Pt/dp-Al<sub>2</sub>O<sub>3</sub> (b). For Pt/dp-Al<sub>2</sub>O<sub>3</sub>, the binding energy of the Pt 4f<sub>7/2</sub> peak was 72.7 eV, which was higher than that reported for Pt<sup>0</sup> (71.4 eV) and lower than that for Pt<sup>2+</sup> (73.6 eV), revealing the ionic Pt<sup>δ+</sup> (0 < δ < 2) nature in the support. What's more, this result indicated the enhanced metal-support interaction due to the electron transformation between metal and supports.

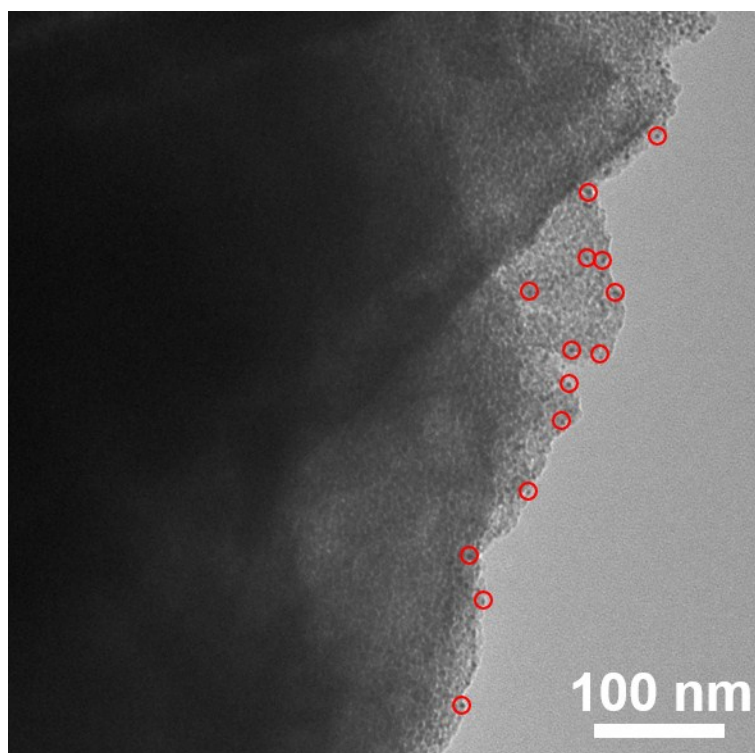


**Fig. S13.** HAADF-STEM images of Pt NPs/c-Al<sub>2</sub>O<sub>3</sub>. It is distinctly observed that plenty of Pt nanoparticles (partially marked by red circles) form on the commercial Al<sub>2</sub>O<sub>3</sub>.

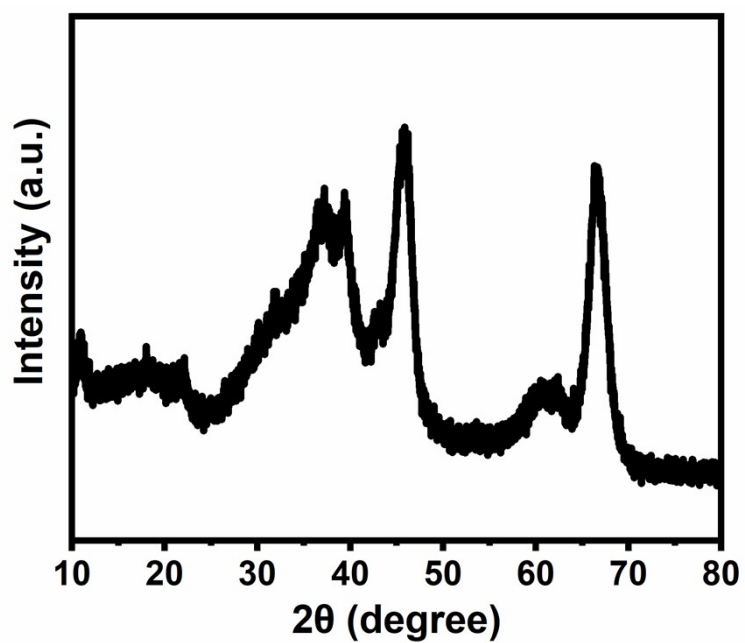


**Fig. S14.** The XRD pattern of the Pt/dp-Al<sub>2</sub>O<sub>3</sub> catalyst after recycle test.

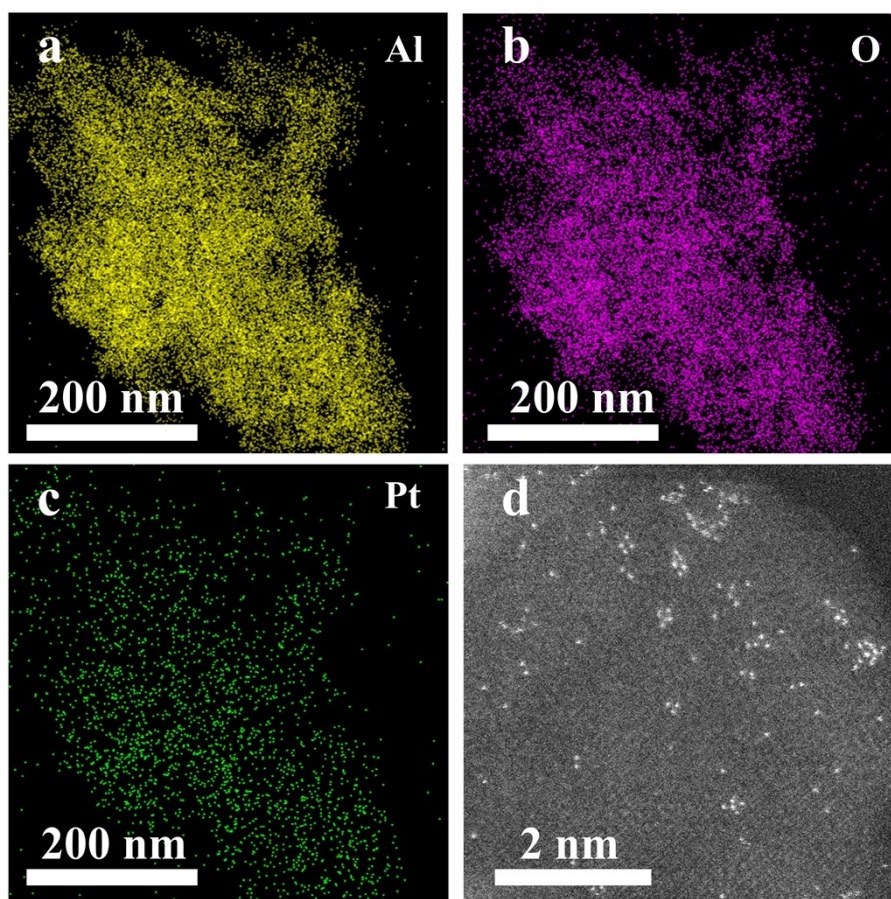


**Fig. S15.** the structural characterizations of the Pt/dp-Al<sub>2</sub>O<sub>3</sub> catalyst after recycle text.  
(a-c) EDS elemental mapping images of Pt/dp-Al<sub>2</sub>O<sub>3</sub> (Al: yellow, O: pink, Pt: green).  
(d) the HAADF-STEM images of Pt/dp-Al<sub>2</sub>O<sub>3</sub>.

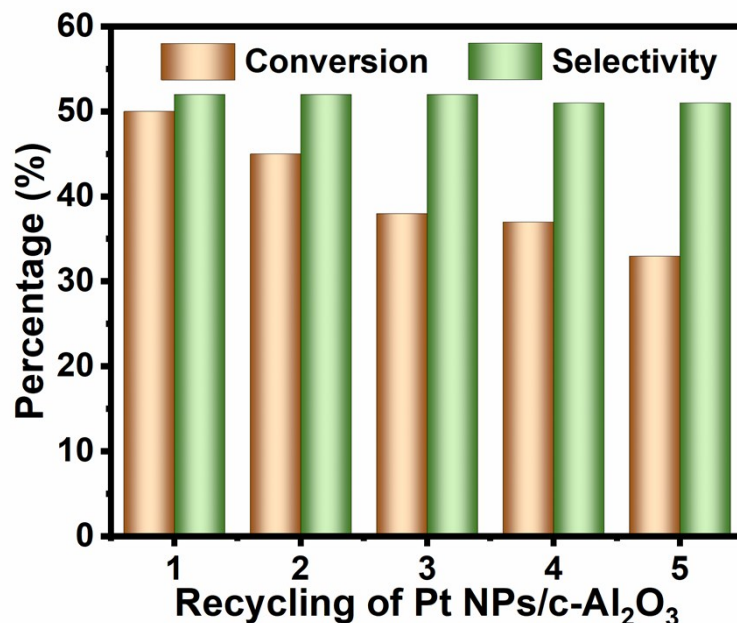
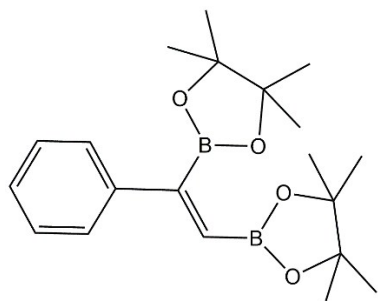


**Fig. S16.** Catalytic performance of Pt NPs/c-Al<sub>2</sub>O<sub>3</sub> for several recycles of repeated reactions.

**Characterization of products.** All products were isolated by flash column chromatography on silica gel with *n*-hexane/ethyl acetate as eluent. The products are characterized by comparison of their <sup>1</sup>H NMR and <sup>13</sup>C NMR spectroscopic data with those reported in the literature. All chemical shifts (δ) are reported in ppm and coupling constants (*J*) in Hz. All chemical shifts were reported relative to tetramethylsilane (0 ppm for <sup>1</sup>H), CDCl<sub>3</sub> (7.26 ppm for <sup>1</sup>H) and CDCl<sub>3</sub> (77.16 ppm for <sup>13</sup>C), respectively.



**(*E*)-2,2'-(1-phenylethene-1,2-diyl)bis(4,4,5,5-tetramethyl-1,3,2-dioxaborolane).** <sup>1</sup>H NMR (400 MHz, CDCl<sub>3</sub>): δ 7.45-7.42 (m, 2H), 7.32-7.28 (m, 2H), 7.25-7.21 (m, 1H), 6.29 (s, 1H), 1.37 (s, 12H), 1.30 (s, 12H); <sup>13</sup>C NMR (101 MHz, CDCl<sub>3</sub>): δ 143.1, 128.3, 127.7, 126.6, 84.2, 83.6, 25.1,

24.9.

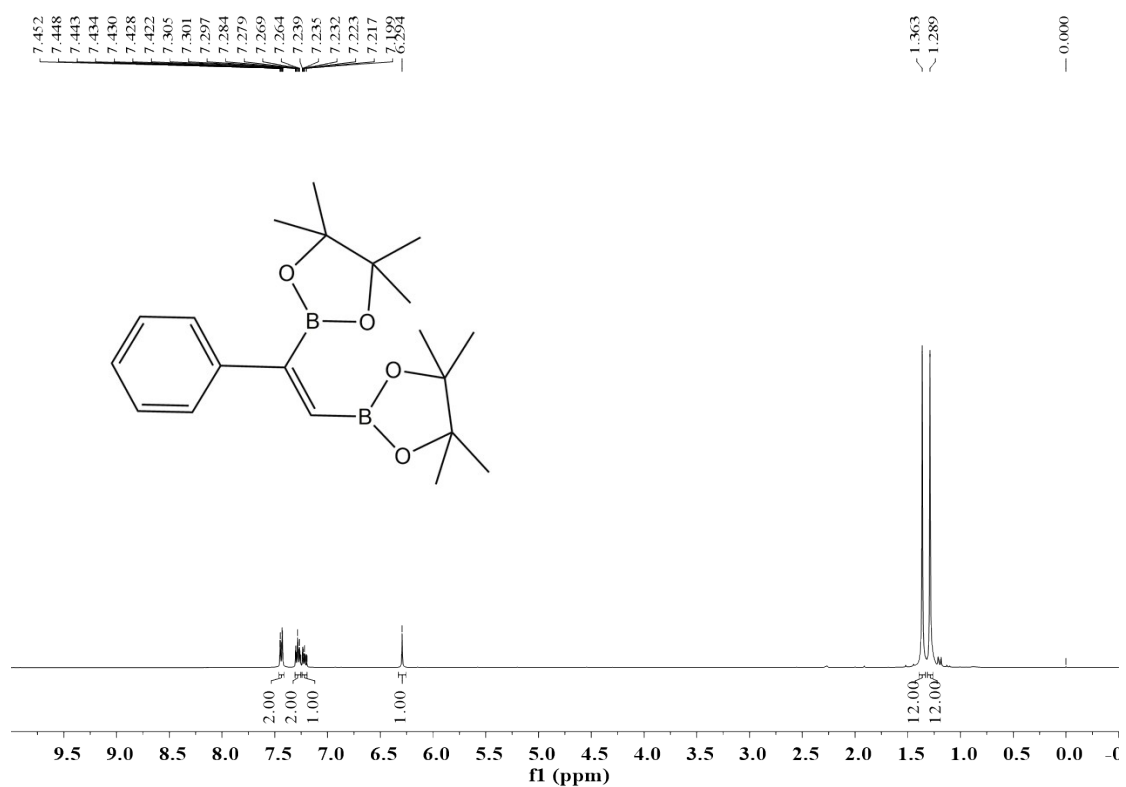


**Fig. S15.** <sup>1</sup>H NMR (400 MHz, CDCl<sub>3</sub>) spectrum of *(E)*-2,2'-(1-phenylethene-1,2-diyl)bis(4,4,5,5-tetramethyl-1,3,2-dioxaborolane).

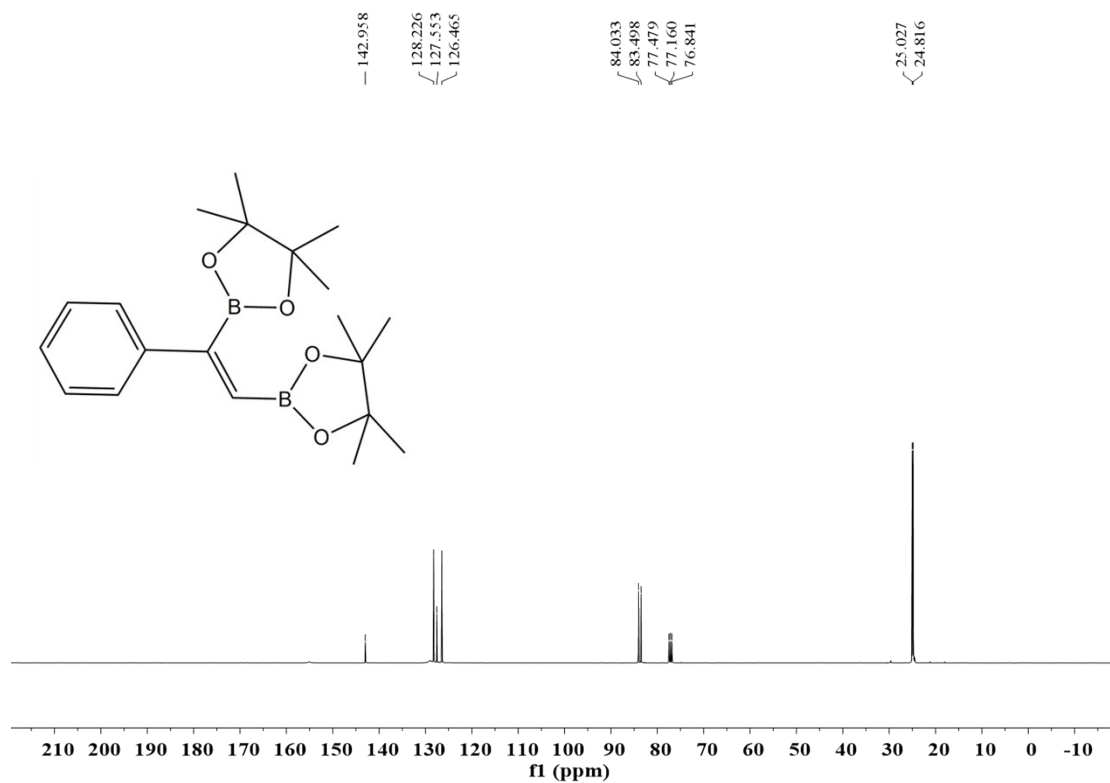


**Fig. S16.** <sup>13</sup>C NMR (101 MHz, CDCl<sub>3</sub>) spectrum of *(E)*-2,2'-(1-phenylethene-1,2-diyl)bis(4,4,5,5-

tetramethyl-1,3,2-dioxaborolane).

**Table S1.** Structural parameters extracted from the Pt L<sub>3</sub>-edge EXAFS fitting. (S<sub>0</sub><sup>2</sup>=0.81)

sample	Scattering pair	CN	R(Å)	σ <sup>2</sup> (10 <sup>-3</sup> Å <sup>2</sup> )	ΔE <sub>0</sub> (eV)	R factor
Pt/dp-Al <sub>2</sub> O <sub>3</sub>	Pt-O	4.1±0.5	2.03±0.01	7.2±0.7	5.2±0.5	0.007
Pt foil	Pt-Pt	12*	2.77±0.01	4.6±0.4	8.2±0.4	0.004

S<sub>0</sub><sup>2</sup> is the amplitude reduction factor; CN is the coordination number; R is interatomic distance (the bond length between central atoms and surrounding coordination atoms); σ<sup>2</sup> is Debye-Waller factor (a measure of thermal and static disorder in absorber-scatterer distances); ΔE<sub>0</sub> is edge-energy shift (the difference between the zero kinetic energy value of the sample and that of the theoretical model). R factor is used to value the goodness of the fitting.

\* This value was fixed during EXAFS fitting, based on the known structure.

Error bounds that characterize the structural parameters obtained by EXAFS spectroscopy were estimated as N ± 20%; R ± 1%; σ<sup>2</sup> ± 20%; ΔE<sub>0</sub> ± 20%.

Pt/dp-Al<sub>2</sub>O<sub>3</sub> (FT range: 2.0-11.6 Å<sup>-1</sup>; fitting range: 1.0-2.4 Å)

Pt foil (FT range: 2.0-13.8 Å<sup>-1</sup>; fitting range: 1.8-3.2 Å)

## References

1. B. Ravel; M. Newville, *Phys. Scr.* 2005, **2005**, 1007.
2. T. Ishiyama, N. Matsuda, N. Miyaura, A. Suzuki, *J. Am. Chem. Soc.* 1993, **115**, 11018-11019.
3. T. Ishiyama, N. Matsuda, M. Murata, F. Ozawa, A. Suzuki, N. Miyaura, *Organometallics* 1996, **15**, 713 -720.
4. A. Grirrane, A. Corma, H. Garcia, *Chem. Eur. J.* 2011, **17**, 2467-2478.

